

ARTICLES

Specific-heat critical behavior of the structural random-field system $\text{Dy}(\text{As}_x\text{V}_{1-x})\text{O}_4$

Z. Slanič, D. P. Belanger, and J. Wang

Physics Department, University of California Santa Cruz, Santa Cruz, California 95064

D. R. Taylor

Department of Physics, Queen's University, Kingston, Canada K7L 3N6

(Received 20 June 1995)

The specific-heat critical behaviors of the pure Ising transition in DyVO_4 and the random-field Ising transition in $\text{Dy}(\text{As}_x\text{V}_{1-x})\text{O}_4$ have been measured. The critical exponent α and amplitude ratio A^+/A^- for DyVO_4 , which has $T_c = 14.82$ K, are in excellent agreement with the known pure $d=3$ Ising exponents. The random fields generated by the local strain fields in $\text{Dy}(\text{As}_x\text{V}_{1-x})\text{O}_4$ depress the transitions to $T_c = 13.45$ K and $T_c = 7.7$ K for $x=0.05$ and $x=0.15$, respectively. With increasing x , the transition becomes rounded and severely depressed in size. The value of α appears large and negative for $x=0.15$. As the random-field strength increases, i.e., the value of x gets larger, the amount of entropy change associated with the transition rapidly decreases. Where the missing entropy reappears is not adequately understood.

I. INTRODUCTION

Although a great deal has been learned about the $d=3$ random-field Ising model (RFIM), major theoretical and experimental puzzles still remain after more than a decade of intense experimental and theoretical investigation. Most of the available experimental data come from studies of diluted antiferromagnets, in particular $\text{Fe}_x\text{Zn}_{1-x}\text{F}_2$, $\text{Mn}_x\text{Zn}_{1-x}\text{F}_2$ (Ref. 1) and $\text{Fe}_x\text{Mg}_{1-x}\text{Cl}_2$.^{2,3} The dilution of the magnetic species leads to random-exchange behavior in zero applied field. In the presence of a field along the ordering axis a crossover to random-field critical behavior is observed with extremely long time dynamics greatly enhanced by the magnetic dilution. Due to the consequent long equilibration times near the transition it is difficult to obtain accurate values of critical parameters in the dilute magnetic systems. Random-field Ising behavior has also been identified in structural systems,⁴ providing an alternative path to exploring the RFIM critical behavior. Long ago Imry and Ma⁵ suggested that structural phase transitions induced by electronic interactions, where crystal defects couple linearly and strongly to the order parameter, could be excellent manifestations of the RFIM. The Jahn-Teller system $\text{Dy}(\text{As}_x\text{V}_{1-x})\text{O}_4$ has been proposed⁶ as an example of a structural RFIM. Pure DyVO_4 and DyAsO_4 undergo tetragonal to orthorhombic phase transitions,⁷ which are believed to be Ising-like, at $T_c = 14.6$ and 11.4 K, respectively. The $\text{Dy}(\text{As}_x\text{V}_{1-x})\text{O}_4$ system has effective short-ranged interactions and has an advantage over dilute magnets in that the active Dy ions are not diluted. Hence this system is an example of a pure RFIM with much less randomness in the interactions and *no vacancies*. The random fields are a result of a size mismatch between As and V ions and the local random environments that lead to local preferences for the distortion direction. This local random ordering field competes with long-range order

in the distortion direction. Several studies have been made to characterize the critical behavior other than that of the specific heat. Birefringence measurements have been done on both pure DyVO_4 and $\text{Dy}(\text{As}_x\text{V}_{1-x})\text{O}_4$ for $x=0.05$ and $x=0.154$ and the exponents β , δ , and γ were determined.⁸ γ for the mixed samples is significantly higher than for the pure samples, but, surprisingly, β remained unchanged. The scaling relation $\gamma = \beta(\delta - 1)$ appears to be satisfied for both pure and random-field samples. The susceptibility critical behavior was also studied in a separate experiment using ultrasonic velocity measurements to monitor the softening of the elastic constant.^{9,10} This study also indicated that the exponent γ increased in the presence of random fields, although agreement with the optical measurements is only fair. This increase in γ , and the assumed validity of the scaling relation $\alpha + 2\beta + \gamma = 2$ led to the prediction⁸ that the specific-heat exponent must go from positive to negative as the As concentration goes from zero to 0.05 and 0.15. Neutron scattering experiments¹¹ and sample capacitance measurements⁶ have also been done in order to characterize the structural phase transition.

II. EXPERIMENTS

Several crystals were used in this study: one with concentration $x=0$ and mass $m=0.1065$ g; one $x=0.05$ and $m=0.3258$ g; one with $x=0.15$ and $m=0.0368$ g; and one with $x=0.15$ and $m=0.54164$ g. Their compositions have been determined previously by a variety of measurements;¹² these also served to show that the compositions are sufficiently uniform to introduce no significant errors into the determination of critical exponents.

The specific heat was measured using an adiabatic heat pulse technique described in more detail elsewhere.^{13,14} The samples were mounted on a sapphire plate using GE7031

varnish. The amount of varnish used and the area of contact between the sample and the varnish was kept to a minimum in order to avoid inducing strain in the sample that could adversely influence the transition properties. The two samples with $x=0.15$, but with greatly different masses, yielded similar results. The similarity of the data for the two samples seems to imply that the mounting strains caused by the varnish are not significant. A small heater on the sapphire plate was used to supply heat pulses using a four wire constant power technique with precisely timed pulses. A bare germanium thermometer was attached to the sample at a point opposite from the point where the sample was mounted to the sapphire plate. The sapphire, sample, and thermometer were then suspended inside the sample chamber with 0.008 mm Be-Cu alloy wires connected to the small heater on the sapphire plate and to the thermometer. The alloy wires provide good electrical conductivity and poor thermal conductivity.

The thermometer attached to the sample generates heat for which compensation is provided by a corresponding heat leak from the sample to prevent temperature drift between pulses. This is accomplished by using two thermometry bridge circuits. One bridge compares the resistances of the germanium thermometers on sample and on the sample chamber. The ratio needed to balance the thermometer heat generation and heat leak to the sample container can be controlled with a heater mounted on the sample chamber neck using the bridge and a heater control feedback circuit. There is an additional germanium thermometer in the neck of the sample chamber, the resistance of which is measured by the second bridge circuit. In equilibrium, the temperature of the sample is higher than that of the sample chamber and the precise amount of heat produced by the thermometer on the sample escapes through the connecting wires from the sample to the sample chamber. When the resistance ratio of one thermometer on the sample chamber and the thermometer on the sample is set to the equilibrium value, the temperature of the system does not drift, i.e., the drift is smaller than 50 μK per minute. The equilibrium bridge ratio (i.e., the temperature difference between the sample and the sample chamber) versus the temperature of the sample chamber is determined before the specific heat measurements commence. The results of the calibration are used by the computer to constantly control the ratio as the sample temperature is increased with the heat pulses. During the experiment, including the time during which the pulse is applied, the system is always kept very close to the equilibrium.

At the beginning of an experimental run, the sample is cooled down to the lowest temperature. The data acquisition process is computer controlled. The small heater on the sapphire plate is given a constant power pulse of 2.3 μW for a period of time corresponding to the desired total heat of the pulse. The total heat pulse used in a typical experimental run corresponds to approximately 100 μJ . Close to the transition, this causes a typical temperature increase of 0.015 K for the $x=0$ sample, which corresponds to a 10^{-3} change in the reduced temperature t , where $t=(T-T_c)/T_c$. For $x=0.05$ and $x=0.15$ samples, the change in the reduced temperature is comparable.

After the heat pulse is applied, the new temperature is measured and the equilibrium value for the ratio is set cor-

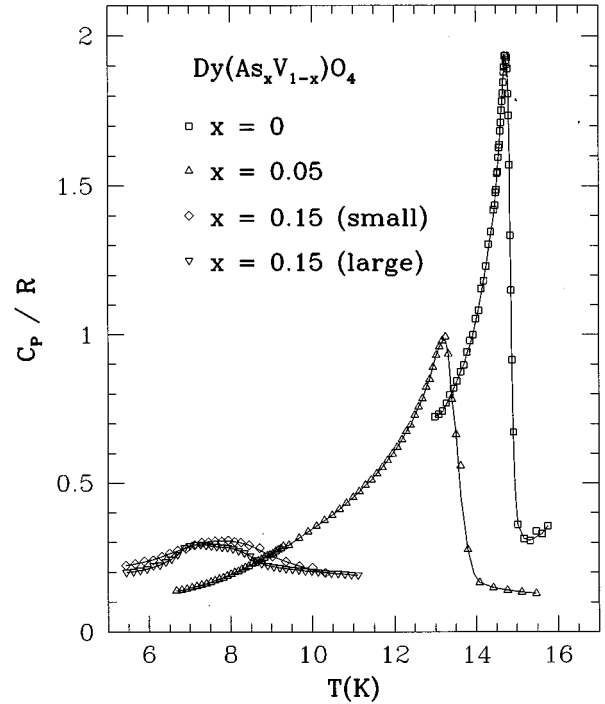


FIG. 1. C_p/R vs T for $x=0$, $x=0.05$, and $x=0.15$ (two samples). For clarity, the points shown in the figure are averages of 2, 4, 3, and 3 heat pulse measurements on $x=0$, $x=0.05$, $x=0.15$ (small), and $x=0.15$ (large) $\text{Dy}(\text{As}_x\text{V}_{1-x})\text{O}_4$ samples, respectively. The lines shown are guides to the eye.

responding to the new temperature. After the measurements are completed, the sample is removed from the sample chamber and the specific heat of the sapphire plate, varnish, and the wires is measured. This background is subtracted from the sample's specific heat before the data are used in fitting or graphing. The advantage of the adiabatic heat pulse method is that it allows a very slow heating process, thus minimizing the effects of dynamics, which can be significant in RFIM systems.

III. EXPERIMENTAL RESULTS

Figure 1 shows C_p/R vs T for all four crystals. [Since the unit cell of $\text{Dy}(\text{As}_x\text{V}_{1-x})\text{O}_4$ contains two Dy ions, there is some ambiguity about what is considered to be a mole of $\text{Dy}(\text{As}_x\text{V}_{1-x})\text{O}_4$. In this paper, a mole is considered to be 6.02×10^{23} Dy ions.] For clarity, the points shown in Figs. 1 and 3 are averages of several heat pulse measurements. Averaging of heat pulses was not used while analyzing the data. In the case of the two $x=0.15$ samples, the small differences between the two sets of data can possibly be attributed to small differences in concentration and to the fact that one sample has an order of magnitude smaller mass, which makes the measurements for that sample more susceptible to systematic errors. Two properties are immediately evident from Fig. 1. First, the transition temperature is greatly depressed by a small amount of mixing and, secondly, the shape and height of the curves change dramatically with increasing x . The total entropy change associated with each

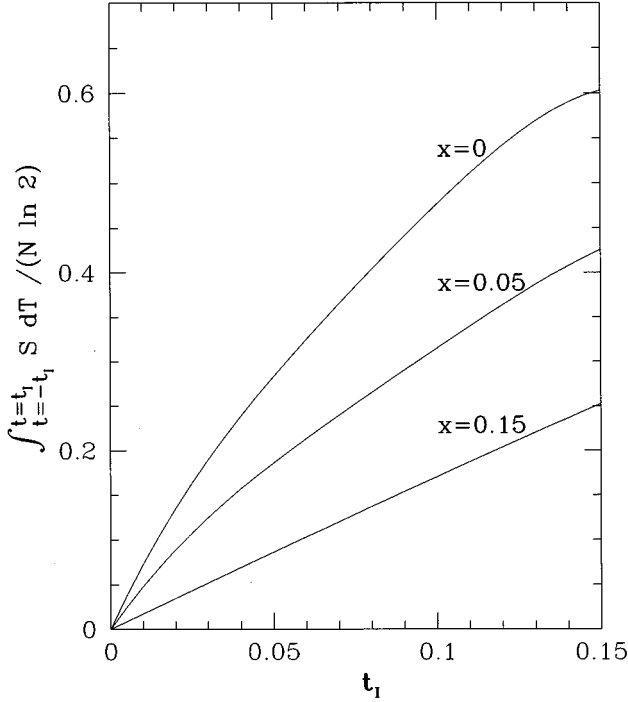


FIG. 2. The percentage of expected entropy change present in the range between $t = -t_1$ and $t = t_1$ vs t_1 for $x=0$, $x=0.05$, and $x=0.15$ Dy(As_xV_{1-x})O₄ samples, where $t = T/T_c - 1$. The amount of entropy change close to the transition temperature decreases dramatically with increasing value of x .

transition is expected to be $N \ln(2)$, where N is the total number of sites that take part in the transition. The entropy change corresponds to the area under the C/T curve. Figure 2 shows the measured entropy as a fraction of the total expected entropy. It is evident that the amount of entropy change close to the transition is decreasing rapidly with increasing x . The background contribution (e.g., phonon contribution) to the specific heat that is not associated with the transition was not subtracted before the entropy integrations were made, leading to an overestimate of our measured entropy.

Figure 3(a) shows C_p/R versus $\log_{10}(|t|)$ (where $t = T/T_c - 1$), as obtained for the pure sample $x=0$. One can observe that the peak is rounded for $t < 10^{-2}$. It should be noted that this rounding of the peak could not be a result of the size of the heat pulse applied to the sample, since a single heat pulse causes a change of only 10^{-3} in reduced temperature. Similarly, the rounding of the $x=0.05$ and $x=0.15$ peaks could not be attributed to the size of the heat pulse.

The $x=0$ sample is expected to exhibit $d=3$ Ising behavior. The curve shown is a fit to the equation

$$C_p = A^\pm |t|^{-\alpha} + B + Et + Ft^2 + Gt^3, \quad (1)$$

where the $+$ and $-$ symbols are for $t > 0$ and $t < 0$, respectively. The solid curve is used in the region in which the data was actually fit to the equation. The nonsingular contributions to the specific heat should be well described by the polynomial background terms. In the fit used in Fig. 3(a)

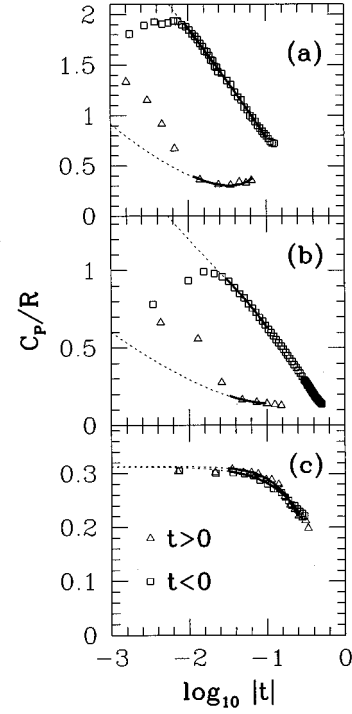


FIG. 3. C_p/R vs $\log_{10}(t)$ for (a) $x=0$, (b) $x=0.05$, and (c) $x=0.15$ (small sample only). For clarity, the points shown are averages of 2, 4, and 3 heat pulse measurements on $x=0$, $x=0.05$, and $x=0.15$ (small) Dy(As_xV_{1-x})O₄ samples, respectively. The solid curves are fits to Eq. (1) using the parameters in Tables I and II. The dotted lines are the continuations of the fitted curves towards $t=0$. Note that the curves were only fitted in the region where the solid curves appear.

only the linear and quadratic background terms were allowed to vary while the cubic term was fixed to zero. The results of this fit for $0.008 < |t| < 0.1$, shown in Table I, agree with experimental and theoretical values determined for the $d=3$ Ising model, also shown in Table I. The values of the universal parameters obtained from fits with cubic background term allowed to vary do not change significantly from those in Table I. We also used correction to scaling terms given in the usual form

$$C_p = A^\pm |t|^{-\alpha} (1 + D^\pm |t|^\nu) + B + Et + Ft^2 + Gt^3 \quad (2)$$

with $x=0.5$. The results of a fit for $0.008 < |t| < 0.1$ are given in Table I. Little change is seen from the fit to Eq. (1). From these fits we see, as expected, that the structural transition does correspond well to the $d=3$ RFIM model in agreement with other experimentally determined critical behavior parameters.⁸ The degree of agreement is perhaps surprising since the fit is over a rather limited range of t .

Figures 3(b) and 3(c) show C_p/R vs $\log_{10}(|t|)$ for the dilute samples with $x=0.05$ and $x=0.15$, respectively. For $x=0.05$ the transition temperature is depressed to 13.45 K, a decrease of 9.2% from the pure sample. A fit to Eq. (1) is indicated by the solid curves in Fig. 3(b). The fit was over the range $0.028 < |t| < 0.1$. This sample shows the characteristic universal critical behavior of the $d=3$ Ising model, as

indicated by the parameters given in Table II. The addition of corrections to scaling, as given in Eq. (2), does not improve the fit substantially. The crossover to RFIM behavior would presumably occur for $|t| < 0.01$. Unfortunately, the rounding of the peak prevented a careful study for $|t| < 0.01$.

C_p/R vs $\log_{10}(|t|)$ for the small crystal with $x=0.15$ is shown along with a fit to Eq. (1) indicated by the solid curves in Fig. 3(c). The exponent and amplitude ratio given in Table II are obtained from fits to Eq. (1) over the reduced temperature range $0.03 < |t| < 0.25$. The peak is nearly symmetric and appears completely rounded, consistent with the large negative value obtained for α . The transition temperature has decreased to 7.7 K, a 48% decrease from the pure system T_c . Hence we are most likely in the large random-field limit.

IV. CONCLUSIONS

We have verified that the specific-heat critical behavior of the pure system DyVO_4 follows the $d=3$ Ising model universality class over the reduced temperature range $0.008 < |t| < 0.1$ investigated in this study. Previous measurements of the specific heat¹⁸ were not detailed enough to establish this fact. The present measurement of α for DyVO_4 taken with previous results for β and γ (Refs. 8,9) (using the average of the two determinations) yields $\alpha + 2\beta + \gamma = 1.98 \pm 0.12$, in good agreement with $\alpha + 2\beta + \gamma = 2$. Hence it is experimentally established that DyVO_4 is an excellent short-ranged interaction Ising model system, although it should be noted that a coupling between the Dy electronic levels and bulk strains is expected to drive the ultimate critical exponents to mean field values.¹⁹

For the mixed samples the specific-heat critical behavior is drastically altered by the random strain fields, but interpretation of the results is not straightforward. The specific heat peak for $x=0.05$ is somewhat rounded and reduced in size relative to the pure sample, but α is almost unchanged. With the results of Ref. 8 for β and γ , we find $\alpha + 2\beta + \gamma = 2.36 \pm 0.13$, in disagreement with the scaling relation. For this concentration, the situation seems to be that γ changed substantially from the pure value,⁸ while α is still the same as for pure DyVO_4 . While unexpected, this result could perhaps be accounted for by crossover effects, where for the range of reduced temperatures accessible experimentally, the random fields control the susceptibility behavior, but not the specific-heat behavior.

For $x=0.15$ the specific-heat is very different, with a peak

TABLE I. The universal critical exponents of DyVO_4 . The data were fit over the range of $0.008 < |t| < 0.1$.

	Fitted values		Theory	Experiment ^a
	Eq. (1)	Eq. (2)		
α	0.13 ± 0.02	0.10 ± 0.04	0.11 ± 0.003^b	0.11 ± 0.005^c
A^+/A^-	0.50 ± 0.06	0.41 ± 0.12	0.55^d	0.54 ± 0.02^b

^aValues obtained from studies of FeF_2 .

^bReference 15.

^cReference 16.

^dReference 17.

TABLE II. The values of the universal parameters for the structural transition of $\text{Dy}(\text{As}_x\text{V}_{1-x})\text{O}_4$ for $x=0.05$ and $x=0.15$.

	α	A^+/A^-	Fitting range
$x=0.05$	0.12 ± 0.02	0.53 ± 0.06	$0.028 < t < 0.1$
$x=0.15$	-1.41 ± 0.10	2.35 ± 0.21	$0.03 < t < 0.25$

that is much reduced and with a rounded, symmetrical appearance. The data are consistent with a substantially negative value of α , but our value must not be considered reliable in view of the strong rounding of the peak. The crossover issue mentioned for the $x=0.05$ sample, and the fact that the specific-heat behavior is so different for the two mixed samples, leave the question open as to what range of compositions would allow the random-field critical exponent α to be determined. There is also the point that, in view of the large decrease in T_c at this concentration, the system is quite possibly in the strong random-field limit. In this limit the system does not necessarily show the critical behavior predicted theoretically for the RFIM, where a small random field is implicit.¹

The striking reduction in the size of the specific-heat peak, indicating a decrease in entropy associated with the random-field transition, is perhaps the most intriguing result of these experiments. Where this entropy reappears is unclear. It may either involve short-range ordering over a large temperature range or a significant amount of disorder remaining to very low temperatures, perhaps in a nonequilibrium configuration. This behavior may simply be a manifestation of cooling in large random fields where, for many sites, the random fields may be greater than the ordering (exchange) field. That this situation could plausibly arise can be seen from the fact that for the 15% As concentrations the majority of Dy sites will have an As impurity as a nearest neighbor. In such cases the remaining entropy change would occur at temperatures well above the transition temperature. If this were the explanation, these sites would not contribute to the structural distortion in the low-temperature phase. Neutron diffraction^{11,21} and optical birefringence measurements²² indicate that the distortion at low temperatures is significantly reduced for $x=0.15$ samples. The observed peak depression is very similar to the peak depression arising in the strongly-diluted antiferromagnet $\text{Fe}_{0.46}\text{Zn}_{0.54}\text{F}_2$,²⁰ when it is cooled in large fields. The ratio of random fields for $\text{Dy}(\text{As}_x\text{V}_{1-x})\text{O}_4$ and $\text{Fe}_{0.46}\text{Zn}_{0.54}\text{F}_2$ systems, calculated from the random-field depression of the transition temperature, is approximately 4. In contrast, the ratio of random-exchange fields for the two systems can be estimated to be approximately 1/4. [The estimate is made from the fact that the transition temperature for $x=0$ and $x=1$ varies by approximately 25% in $\text{Dy}(\text{As}_x\text{V}_{1-x})\text{O}_4$, whereas the corresponding variation in $\text{Fe}_{0.46}\text{Zn}_{0.54}\text{F}_2$ is 100%.] Even though the ratio of random to exchange fields is different for the two systems, they show a very similar behavior. The temperature derivative of the optical birefringence is depressed and rounded when $\text{Fe}_{0.46}\text{Zn}_{0.54}\text{F}_2$ is cooled in large fields, similar to the strong peak depression in the case of $\text{Dy}(\text{As}_{0.85}\text{V}_{0.15})\text{O}_4$. In $\text{Fe}_{0.46}\text{Zn}_{0.54}\text{F}_2$ it is probable that the major sources of the depressed specific heat are dilution of the magnetic ions and the consequent slow

equilibration. These should not be significant in $\text{Dy}(\text{As}_{0.15}\text{V}_{0.85})\text{O}_4$, where the active ions are not diluted and the equilibration times are no more than seconds,⁶ at least down to T_c .

While this structural system has attractive features in terms of the study of RFIM behavior, serious puzzles remain in the critical properties of this system. On the one hand, the susceptibility exponent γ increases substantially from that of the pure system, and agrees reasonably well with antiferromagnetic systems.²³ On the other hand, the order parameter exponent β seems to remain unchanged, and the determination of α is problematical because of possible crossover complications and a dramatic loss in entropy of ordering. In

diluted antiferromagnetic systems, $\alpha \approx 0$ appears to be a robust value for the specific-heat exponent and the order parameter measurements²⁴ in the dilute antiferromagnets are not well understood at this time. Thus, despite the progress in characterizing the specific heat critical behavior, the experimental situation for the critical properties of the RFIM is still unsettled.

ACKNOWLEDGMENTS

This work was supported in part by the DOE Grant No. DE-FG03-87ER45324 and by the Natural Sciences and Engineering Research Council of Canada.

-
- ¹D. P. Belanger and A. P. Young, *J. Magn. Magn. Mater.* **100**, 272 (1991).
- ²U. A. Leitão and W. Kleemann, *Phys. Rev. B* **35**, 8696 (1987).
- ³W. Kleemann, B. Igel, and U. A. Leitão, *New Trends Magn.* **26-28**, 85 (1990).
- ⁴W. Kleemann, *Int. J. Mod. Phys.* **7**, 2469 (1993).
- ⁵Y. Imry and S. K. Ma, *Phys. Rev. Lett.* **35**, 1399 (1975).
- ⁶J. T. Graham, M. Maliepaard, J. H. Page, S. R. P. Smith, and D. R. Taylor, *Phys. Rev. B* **35**, 2098 (1987).
- ⁷G. A. Gehring and K. A. Gehring, *Rep. Prog. Phys.* **38**, 1 (1975).
- ⁸K. A. Reza and D. R. Taylor, *Phys. Rev. B* **46**, 11 425 (1992).
- ⁹J. T. Graham, J. H. Page, and D. R. Taylor, *Phys. Rev. B* **44**, 4127 (1991).
- ¹⁰H. M. Elmehdi, J. H. Page, and J. T. Graham, *J. Magn. Magn. Mater.* **104-107**, 193 (1992).
- ¹¹J. T. Graham, D. R. Taylor, D. R. Noakes, and W. J. L. Buyers, *Phys. Rev. B* **43**, 3778 (1991).
- ¹²D. R. Taylor *et al.*, *J. Phys. Chem. Solids* **51**, 197 (1990).
- ¹³J. Wang, D. P. Belanger, and B. D. Gaulin, *Phys. Rev. B* **49**, 12 299 (1994).
- ¹⁴J. Wang, Ph.D. thesis, UCSC, 1994.
- ¹⁵J. C. Le Guillou and J. Zinn-Justin, *Phys. Rev. Lett.* **39**, 95 (1977).
- ¹⁶D. P. Belanger, P. Nordblad, A. R. King, V. Jaccarino, L. Lundgren, and O. Beckmann, *J. Magn. Magn. Mater.* **31-34**, 1095 (1983).
- ¹⁷E. Brezin, J. C. Le Guillou, and J. Zinn-Justin, *Phys. Lett.* **47A**, 285 (1974).
- ¹⁸A. H. Cooke *et al.*, *Solid State Commun.* **8**, 689 (1970).
- ¹⁹J. H. Page, D. R. Taylor, and S. R. P. Smith, *J. Phys. C* **17**, 51 (1984).
- ²⁰I. B. Ferreira, A. R. King, and V. Jaccarino, *Phys. Rev. B* **43**, 10 797 (1991).
- ²¹D. R. Taylor, K. A. Reza, and J. T. Graham, *Phys. Rev. B* **52**, 7108 (1995).
- ²²D. R. Taylor and K. A. Reza, *J. Phys. Condens. Matter* **6**, 10 171 (1994).
- ²³D. P. Belanger, A. R. King, and V. Jaccarino, *Phys. Rev. B* **31**, 4538 (1985).
- ²⁴D. P. Belanger, J. Wang, Z. Slanič, S.-J. Han, R. M. Nicklow, M. Lui, C. A. Ramos, and D. Lederman, *J. Magn. Magn. Mater.* **140-144**, 1549 (1995).